Category: STEM (Science, Technology, Engineering and Mathematics)

ORIGINAL

Effect of Friction Stir Processing Parameters on Microstructure and Mechanical Properties of Aluminum Alloy AA6061-T6: Experimental and Statistical Study

Efecto de los parámetros de procesado por fricción en la microestructura y propiedades mecánicas de la aleación de aluminio AA6061-T6: Estudio experimental y estadístico

Khaldoon K. Jlood[1] ✉, Muna K. Abbass[1] ✉, Mahdi M. Hanoon[1] ✉

[1]Production Eng. and metallurgy. Dept, University of Technology. Baghdad, Iraq.

ABSTRACT

The current study investigates the effects of friction stir processing (FSP) parameters on the mechanical and microstructural characteristics of the alloy AA6061-T6. The FSP's big-area stir zone is where the fine-equiaxed grains are created, and it was found that the size of the grain of every pass is homogenous there. The design of experiment (DOE) method has been used to identify the key variables affecting the final tensile strength. FSP was accomplished using threaded cylindrical pin profiles with three varying rotational speeds (930, 1100, and 1460 rpm) and various transverse speeds (23, 50, and 79), and the tilt angle of the tool was also set at 2°. The optimum FSP parameters were two passes at 1460 rpm and 79 mm/min with these values. It was found that the stir zone's center has a greater microhardness value of 235 kg/mm^2 at three passes and that this value decreased toward the thermomechanically affected zone (TMAZ), HAZ, and base metal (107 kg/mm2). The result showed that the FSPed sample has a higher tensile strength at two passes than at one or three passes. Also, it was obtained from the ANOVA analysis results that travel speed is the most effective factor, giving 51,46 % of the contribution feature pursued by No. of Pass (22,56 %), followed by rotational speed (19,49 %).

Keywords: Friction Stir Processing; AA6061-T6 Alloy; Taquchi Technique; Mechanical Properties.

RESUMEN

El presente estudio investiga los efectos de los parámetros del proceso de agitación por fricción (FSP) sobre las características mecánicas y microestructurales de la aleación AA6061-T6. La zona de agitación de gran superficie del FSP es donde se crean los granos finos equiaxiales, y se ha comprobado que el tamaño del grano de cada pasada es homogéneo allí. Se ha utilizado el método de diseño de experimentos (DOE) para identificar las variables clave que afectan a la resistencia final a la tracción. La FSP se realizó utilizando perfiles de pasador cilíndrico roscado con tres velocidades de rotación variables (930, 1100 y 1460 rpm) y varias velocidades transversales (23, 50 y 79), y el ángulo de inclinación de la herramienta también se fijó en 2°. Con estos valores, los parámetros óptimos de FSP fueron dos pasadas a 1460 rpm y 79 mm/min. Se observó que el centro de la zona de agitación tenía un valor de microdureza mayor de 235 kg/mm2 en tres pasadas y que este valor disminuía hacia la zona afectada termomecánicamente (TMAZ), la HAZ y el metal base (107 kg/mm2).

El resultado mostró que la muestra FSPed tiene una mayor resistencia a la tracción a dos pasadas que a una o tres pasadas. Asimismo, se obtuvo de los resultados del análisis ANOVA que la velocidad de desplazamiento es el factor más eficaz, aportando el 51,46 % de la contribución característica perseguido por el n° de pasadas (22,56 %), seguido de la velocidad de rotación (19,49 %).

Palabras clave: Procesado por Fricción-Agitación; Aleación AA6061-T6; Técnica Taquchi; Propiedades Mecánicas.

INTRODUCTION

Due to their light weight and high strength-to-weight ratio, aluminum alloys are crucial for numerous applications in the aerospace and automotive sectors, among others. The aluminum alloy 6061-T6 is extensively used in marine environments, automobiles, and aircraft due to its advantageous properties, which include its virtuous strength, virtuous corrosion and erosion properties, and light weight.[1,2] The grain structure of the alloy can be homogenized and refined to improve its mechanical characteristics. It can be done using a variety of techniques, including the equal channel angular process (ECAP), accumulative roll bonding (ARB), high pressure torsion (HPT), thermal mechanical treatment (TMT), and so on. It takes a lot of time and effort to complete this.[3,4] Recently, a novel method called Friction Stir Processing (FSP) has been created for the production of surface composite materials and grain refinement. It shares many of FSW's fundamental tenets. FSP is a very hopeful technique for improving metal properties. High strain rates and significant plastic distortion are the results of this process.[5] To alter the surface properties of metals and composites, various surface treatments have been used. These techniques can be used for a variety of purposes, including ornamentation, reflectivity, increased hardness, increased wear resistance, and corrosion protection. FSP is one of these techniques that show promise because it sharpens the surface microstructure through significant localized plastic distortion (i.e. severe plastic deformation). In this technique, a non-consumable tool is moved laterally through the thickness of the workpiece while being rotated in a stirring action.[6,7,8] FSP has many advantages. It's a single-step, short-route solid-state technique that performs uniformity as well as microstructural refinement. Additionally, the heat intake during FSP is caused by friction and plastic deformation, indicating that this method is both environmentally and energy-friendly and free of harmful gases, radiation, and noise.[9]

FSP concentrates the changes and controls of microstructures in the metal component's processed near-surface layers. Taguchi technique has been extensively used in engineering analysis and in the design of high-quality systems for examining the FSP parameters impact using a limited no. of tests.[10] Shafiei Zarghani et al.[11] used the FSP to rigidly deform materials into very tiny grains. FSP has been utilized for extruding the aluminum alloy (AA6082-T4) for producing a microstructure with too tiny grains that range in size from 0,5 mm to 3 mm. When the rotational speed of the tool is slowed down, the hardness of the FSPed aluminum alloy improves significantly.

Magdy et al.[12] employed FSP for altering the microstructure as well as improving the tensile characteristics of the aluminum alloy (AA6082-T6). The processing was conducted at a fixed rotational speed of 850 rpm and various traverse rates of (90, 140 and 224 mm/min). As the traverse speed was raised, the hardness and strength increased; however, as the no. of passes was increased, a softening and a reduction in the final tensile strength increased.

Muna et al.[13] investigated the optimization of FSP parameters which influence upon the tensile strength of aluminum alloy (AA6061-T6) utilizing the Taguchi method. The FSP was carried out at various transverse speeds (16, 25, and 32 mm/min), various rotational speeds (800, 1000, and 1250 rpm), and no. of passes (1, 2, and 3) in the similar direction, and a (2°) tilt angle of tool utilizing a threaded cylindrical pin profile. Results showed that the best parameters of FSP were (32 mm/min transverse speed), (1250 rpm rotational speed), and (2) passes.

Namdev Ashok Patil et al.[14] studied the optimization of FSP factors to improve the surface properties of AA7075-SiC/Gr hybrid surface composites. And, three traverse speeds (20, 30, 40 mm/min), three rotational speeds (500, 1000, and 1500 rpm), strengthening particles hybrid ratios (60:40, 75:25 and 90:10), and three volume percentages (4 %, 8 % and 12 %) were utilized as independent factors. Also, the influence of such factors upon the microstructure, micro hardness, and wear characteristics of the surface composites were investigated. Additionally, the factors' significance and their interactions to maximize the hardness and minimize both the rate of wear as well as the coefficient of friction (COF) were obtained.

Muna et al.[15] investigated the FSP influence upon the mechanical properties and microstructure of TIG welded aluminum alloy (AA 2024T3) by utilizing 4043 filler metal. It was found that joint efficiency, tensile strength, and hardness increased after the FSP over the welded joint.

The current research objective is to determine the best FSP parameters, which are the travel speed, tool rotational speed, and no. of passes as well as studying their influence upon the microstructures and mechanical

properties of AA6061-T6 alloy. L9 Taguchi orthogonal array has been used for identifying the most efficient parameters of FSP. Analysis of variance (ANOVA) has also been employed for to determining the relative importance of every parameter to the procedure.

The aim of the research

Optimization of the friction stir processing parameters (rotational speed, travel speed, and number of passes) depending on the tensile strength of AA6061-T6 aluminum alloy will be adjusted using the Taguchi technique and design of experiments (DOE).

Experimental Methods

In this research, the aluminum alloy plate AA6061-T6 with a thickness of 6 mm was used. Using a cutting machine, such a plate was cut into measurements of 150 x 100 mm. As shown in table 1, the chemical composition of this alloy was determined using a spectro-meter analysis tool that was made by "ALNABAA CO. ENGINEERING SERVICES." And the mechanical properties of the AA6061-T6 alloy are shown in table 2.

Table 1. The chemical composition of the used (AA6061-T6) alloy (wt.%)								
Element wt.%	Al	Si	Fe	Cu	Mn	Mg	Cr	Zn	Ti
Standard value	95-98	0,4-0,8	0,7	0,15- 0,4	0,15	0,8-1,2	0,04-0,35	0,25	0,15
Measured value	96,7	0,7	0,52	0,38	0,05	0,80	0,12	0,04	0,018
T6: Solution heat treatment and artificial aging								

Table 2. The mechanical properties of the used (AA6061-T6) alloy				
Base alloy	Yield Strength (MPa)	Tensile Strength (MPa)	Elongation (%)	Hardness (HV)
Standard value	276	296	25	107
Measured value	190	322	28	110
*Datasheet for the ASM Aerospace Specification Metals Inc				

FSP was carried out using a vertical milling machine (Type WMW-Heckert, Germany). As shown in figure 1, the specimens are produced, held in a particularly made fixture, and tightly clamped to guarantee that the plates stay in position as well as don't move away due to the forces of FSP. The tool was then inserted into the selected sheet area. High-speed steel (H13) cylindrical-shouldered and threaded pins with a non-consumable shoulder diameter of 16 mm, a (6 mm) pin diameter having a length of 3,2 mm, and a (2°) tool inclination angle were used. Figure 2 presents the FSP sample at (R.S. = 1460, T.S. = 79, and No. of Pass = 1).

Figure 1. Sample after FSP

Figure 2. FSP sample at (R=1460, T=79, and P=1)

Specimens, which were created from a FSP cross section in a series of steps, were tested employing an optical microscope. The water and SiC emery papers in different grits (400, 500, 600, 800, 1000, and 1200) were used in the wet grinding procedure. A (0,5 μm) paste of diamond, a specific polishing cloth, and lubrication were utilized to polish the samples. The etching process for specimens was done by employing Keller's reagent consisting of 1,0 ml HF, 1,5 ml HCL, 2,5 ml HNO3, and 95 ml H2O for 10 to 30 seconds. The specimens were then cleaned and dried. The Vickers hardness tester type (TH714) was utilized for conducting the test of Vickers hardness. The sample's hardness was measured using a 200-gram load for 15 seconds. The hardness of each sample was measured five times, and the average hardness was calculated. Figure 3 manifests the specimen preparation for the mechanical tests (hardness test, microstructure test, and tensile test).
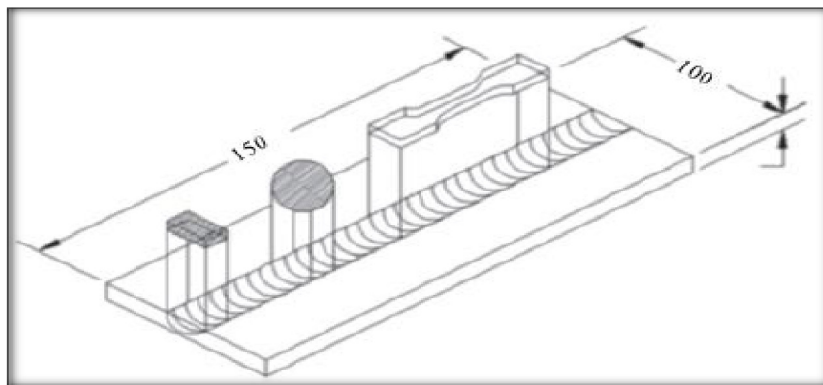

Figure 3. Specimen preparation for mechanical test (A=hardness test, B= microstructure and C= tensile test)

Taguchi Technique
To organize the FSP parameters as well as the levels at which they have to vary in order, Taguchi's experimental plan uses orthogonal arrays. Three tests were run on each set of the parameters of the process using the (L9) orthogonal array (3*3) proposed by the Taguchi technique. The rotational speeds (rpm), transversal speeds (mm/min), and number of passes in a similar direction were used in this study. The process parameters and stages are displayed in table 3. The tilt position (2o) was fixed. Nine experimental runs were performed in total, and each control factor was subjected to a set of levels, as evinced in table 4.

Table 3. The used FSP parameters with their level			
Parameter	**Level 1**	**Level 2**	**Level 3**
Rotation speed, RS (rpm)	930	1100	1460
Travel speed, T.S (mm/min)	23	50	79
No. of passes, No. P	1	2	3

Table 4. The experimental results of the DOE Taguchi (L9) Orthogonal array			
No. of Experiment	**C1**	**C2**	**C3**
	R.S	**T.S**	**No. P**
1	930	23	1
2	930	50	2
3	930	79	3
4	1100	23	2
5	1100	50	3
6	1100	79	1
7	1460	23	3
8	1460	50	1
9	1460	79	2

Tensile tests were carried out following the friction stir processing to determine the FSP tensile strength at the whole processing parameters. The tensile specimens were sliced longitudinally parallel to the FSP using a CNC Water jet Cutting Machine (C-WJCM). And, the tensile specimen's shape and dimensions are displayed in figure 4 in accordance with the characteristics listed in the ASTM standard (E8M- 011) for the sub-size specimens.[13]
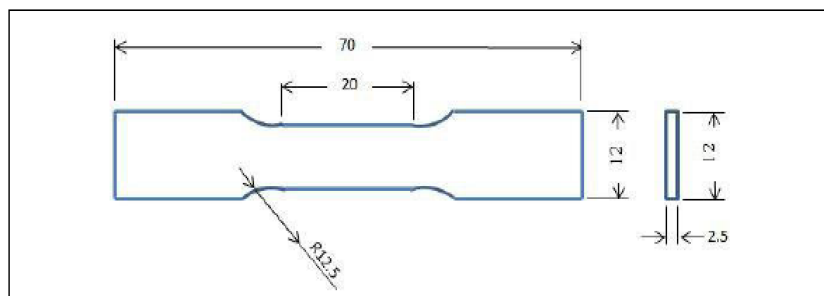

Figure 4. ASTM standard (E8/E8M-011) tensile test specimen (All dimensions are in mm)

RESULTS AND DISCUSSION

Signal to noise (S/N) ratio

The essential feature considered in the present study is the tensile strength. The means and S/N ratio values for each of the direct factors (travel speed, tool rotational speed, and no. of passes) were taken into consideration for the FSP parameters' impact assessment upon the tensile strength. Using prior knowledge, experience, and an understanding of the process, a suitable S/N ratio was chosen. For maximizing the response, the signal to noise (S/N) ratio for this study was selected carefully using the standard that the greater is better. The S/N ratio is used in Taguchi's approach to calculate the difference between the desired value and the quality attributes. Tensile strength data were studied in this work to determine the impact of FSP parameters. The strength means as well as the corresponding (S/N) ratio are shown in table 5 together with the (3) levels of process parameters as "per L9 orthogonal array". In order to ensure the high tensile strength levels in terms of the investigational data, the analysis of mean for each experiment will lead to superior parameter combination levels. The graphs shown in figures 5 and 6 can be utilized for determining the parameter of process that is most in line with the uppermost tensile strength and (S/N) ratio. According to the means and (S/N) ratios plots, 1460 rpm rotational speed, 79 mm/min travel speed, and (2) no. of passes produce the highest tensile strength.

Table 5. The tensile strength and signal to noise (S/N) ratio for the experiments					
No. of Experiment	**C1**	**C2**	**C3**	**C5**	**C.6**
	R.S (rpm)	**T.S (mm\min)**	**No. P**	**S/N Ratio**	**MEAN T.S MPA**
1	930	23	1	43,2274	145
2	930	50	2	43,5795	151
3	930	79	3	43,2274	145
4	1100	23	2	42,7344	137

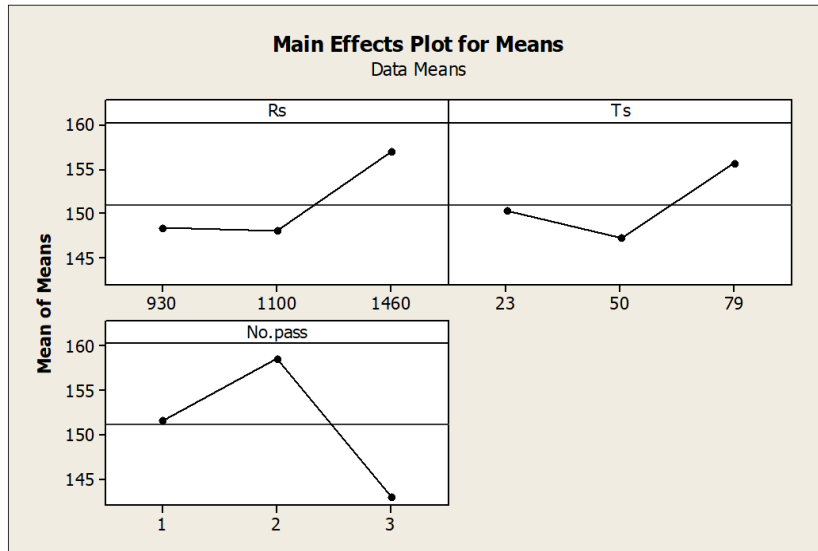| 5 | 1100 | 50 | 3 | 43,2871 | 146 |
6	1100	79	1	44,1365	161
7	1460	23	3	42,9844	141
8	1460	50	1	44,0824	160
9	1460	79	2	44,6090	170

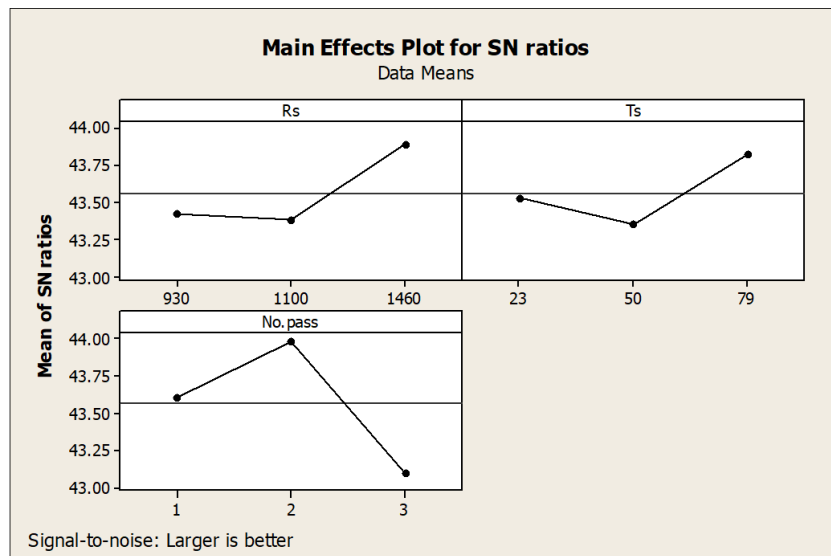**Figure 5.** Main Effects plots for means

Figure 6. Main Effects plot for SN ratios

Tensile test results

Results of tensile test elucidated that the tensile strength of base alloy exceeded that of every friction stir processing method that was evaluated figure 7. The test findings indicate that increasing the travel and rotation rates will increase the tensile strength and the tensile strength was the highest at (1460 rpm) tool rotation speed. Also, it was found that the higher tool rotational speed produces a decrease in the tensile strength when compared to the untreated alloy. This is due to the excess heat created in the stir region by increasing the speed of rotation, which increases the stirring impact associated to the pin, but it may also result in further explosion or metal flowing in form of flash outside, generating flaws in the stir region. Likewise, increasing the heat input is going to boost the peak temperature and accelerate the grain growth, lowering the tensile strength.

At travel speeds of (23 mm/min) and (50 mm/min), the tensile strength was found to be lower than at speed (79 mm/min), which is attributed to the enhanced heat of friction as well as the dissipation of the majority of the heat generated independent of the tool rotational speed and number of passes. Due to the highest heat input into processing the specimens, the minimum rotational speed results in a reduction in the tensile strength

of FSP, where the maximum rotational speed creates an increase in the tensile strength, causing a short time of exposure to the heat of friction.

The FSP has a higher tensile strength at two passes than at a single or (3) passes. And, this is due to that the FSP has a noticeable impact on the intermetallic compound's breakdown and refining of the stir zone microstructure after two passes. The best FSP tensile strength result was obtained with two passes at (79 mm/min) rotational speed (1 460 rpm). The observed outcomes are in agreement with the Magdy et al.[16] findings.
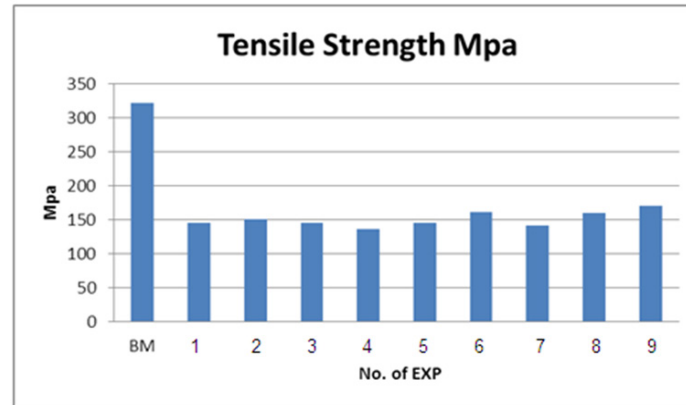

Figure 7. The tensile strength of (AA6061-T6) base alloy and FSP specimens

Analysis of variance (ANOVA)

This analysis was used to investigate the FSP parameters' significance influencing the tensile strength associated with FSP treating. And, the F-test, called after Fisher, may be employed for evaluating which procedure significantly affects the tensile strength. Generally, when the (F) value being high, the difference in process parameter possesses a significant impact upon the quality traits connected to the tensile strength of processing. Findings of the ANOVA analysis revealed that the process parameters, specifically the number of passes, travel, and rotation speeds, possess a significant influence upon the FSP tensile strength. Table 6 lists the ANOVA results of the tensile test and demonstrates that the rotational speed, with a contribution percentage of 19,49 %, is the highly influential parameter, pursued via the no. of passes (22,56 %) and travel speed (51,46 %).

Table 6. Lists the ANOVA				
Parameter	Dof	Ss	Ms	P%
Rs	2	182	91	19,49
Ts	2	480,7	240,3	51,46
No. pass	2	211	105	22,56
Error	8	51,3		5,5
Total		934		100

The regression equation is
T.S = 123 + 0,0198 Rs + 0,314 Ts - 5,67 No.pass

Microhardness Results

Microhardness test was performed on cross section of FSP plates using Vickers hardness tester. The measured hardness values are taken for on and two pass over FSP zone on both slides (advancing and retreating) on different znes SZ, TMAZ, HAZ and base alloy. FSP zone show similar distributing of hardness over four zone for both pass but the second pass exhibited higher hardness than one pass. Distribution of the microhardness over the cross section of FSP in figure 8 depicts the Vickers-microhardness distribution upon the cross section perpendicular to the traverse direction of the tool for the FSP specimen produce at a (1 460 rpm) tool rotational speed, a (79 mm/min) travel speed, and (1), (2) and (3) passes. And, the unaffected zone is softer than the stir zone. The measured hardness values are taken for one, two, and three passes over FSP zones on both slides (advancing and retreating) on different znes SZ, TMAZ, HAZ and base alloy. FSP zone show similar distributing of hardness over four zone for both passes but the three pass exhibited higher hardness than that of one and two passes. This is caused by grain refining, the dynamic re-crystalline of stir region, and the existence of the 2nd precipitates of Al_3Mg_2 phase in α-Al. It can be seen that HAZ shows drop in hardness reaching the base alloy (AA6061), this is due to dissolving of the metastable percipitates (Al_3Mg_2) lead to decrease in the hardness of HAZ.
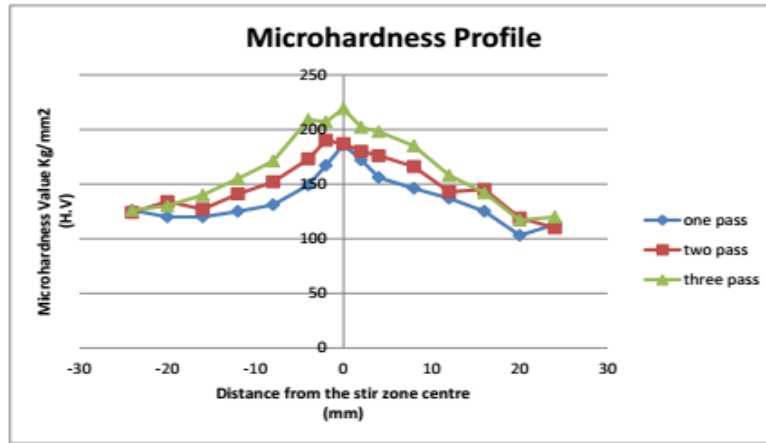
Figure 8. Hardness distribution over the cross section of FSP specimen at 1460 rpm and 79 mm/min for (AA6061-T6) alloy

The microhardness results portrayed that the higher values of hardness were found in the nugget zone's (NZ) center and progressively decreased throughout the thermo-mechanically-affected zone (TMAZ) and the heat-affected zone (HAZ) toward the base metal. The hardness surface AA6061 alloy was significantly influenced by the FSP processing factors. When using multi-pass FSP, the findings of the microhardness analysis are also influenced by the speed of travel.[17] The results show increase as No of passes increased. This is due to the refine grains in stir zone in two pass greater than one pass. As shown by a tool travel speed of 79 mm/min, the improvements in the tool travel speed reduce the effects of heat produced and shorten the exposure times.[18]

Microstructure results
The microstructural analysis of a friction stir processing cross section is viewed in figure 9 and 10 at the optimal conditions (1 460 rpm, 79 mm/min, and 2 cycles). The FSP sample can be seen to have four different regions: Stir Zone (SZ), which is the thermo-mechanically processed region where the size of grain is too fine and the grains have an equalized or uniform structure, The FSP Zone and the Thermo-Mechanically Affected Zone (TMAZ) are other Thermo-mechanically processed zones where the grain is elongated as a result of being thermo-mechanically deformed with the observation of union rings, The area that is not affected by the FSP process is considered to be the base metal (BM) or the (AA6061-T6) alloy (the unaffected metal), which being regarded to possess the similar structure of grain as the BM. This microstructure has an evenly dispersed second-phase particles that being very finely precipitated into the α-Al. Figure 11 represent the FE-SEM for FSPed composite sample at different magnifications.
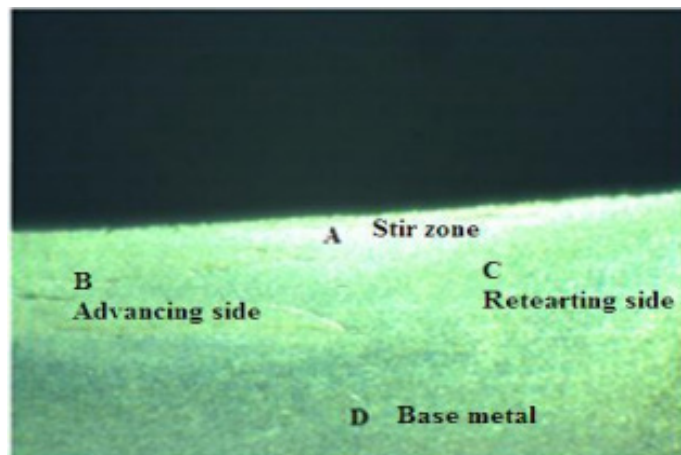
Figure 9. The Microstructure of the FSP specimen at the optimal conditions (1460 rpm , 79mm/min, and 2 passes) comprising: (a) ST, (b) TMAZ in advancing side, (c) TMAZ in retearting side, and (d) BM
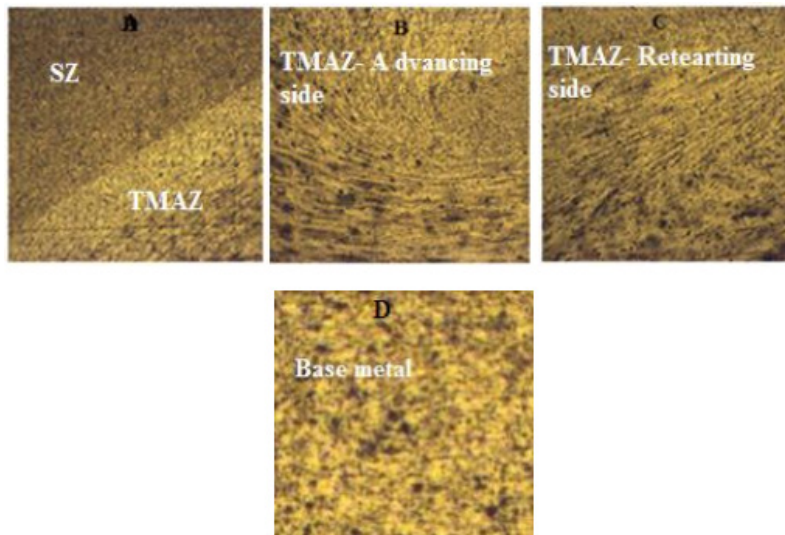
Figure 10. Optical micrograph showing the microstructure of the FSP specimen at the optimal conditions (1460 rpm , 79mm/min, and 2 passes) comprising: (a) ST, (b) TMAZ in advancing side, (c) TMAZ in retreating side and (d) base metal at 400X
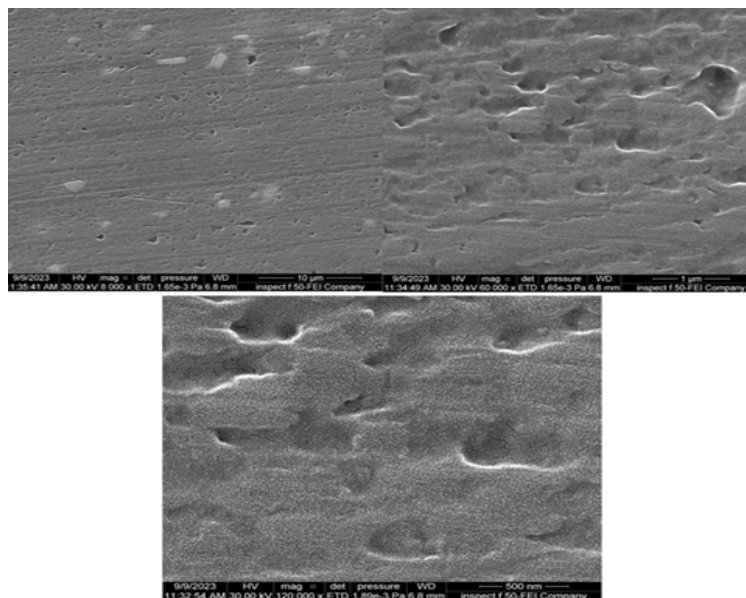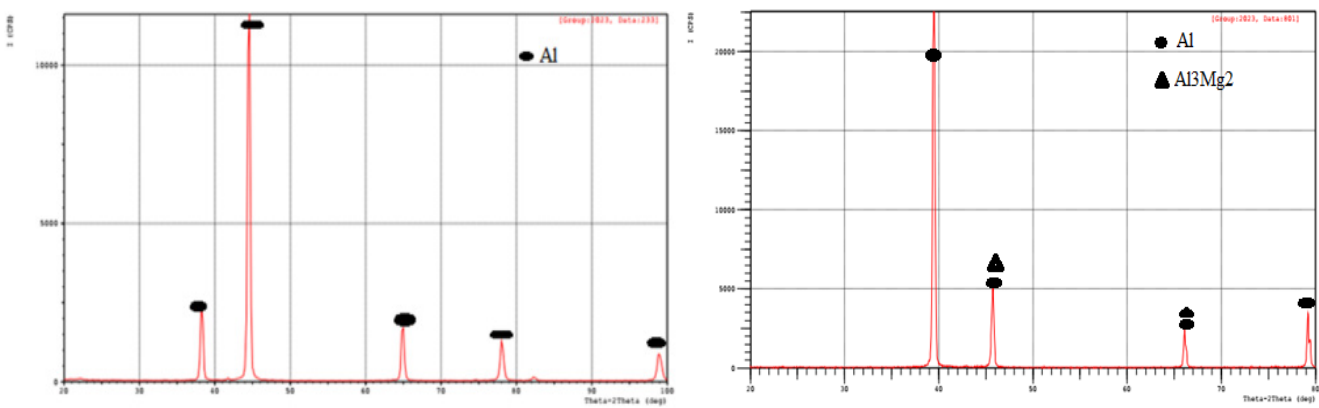

Figure 11. FE-SEM micrograph for FSPed composite sample at optimum conditions in stir zone

A- XRD analysis for base metal   B- XRD analysis for FSPed composite sample
Figure 12. XRD analysis of (a) base metal and (b) FSPed composite sample

It was seen that Al peaks are found which represent the α-Al matrix, while the 2θ angles of precipitates phase of Al_3Mg_2 apparent at same angles of α-Al matrix. This is due to heat treatable alloy AA6061-T6 that contains α-Al and pptes. The XRD patterns of base alloy and composite samples after friction stir processing

under ideal conditions are clarified in figure 12.

CONCLUSIONS

1. The optimum or best parameters of FSP were found at a rotational speed of 1460 rpm, a travel speed of 79 mm/min, and a number of (3) passes.

2. The FSP stir zone manifested a higher microhardness than HAZ and TMAZ.

3. The tensile strength of the FSPed specimen rose as both the rotational and travel speeds were increased.

4. It was shown that multipass in FSP increased the hardness of SZ and TMAZ in both slides (advancing and retreating).

5. It was seen that Al peaks are found, which represent the α-Al matrix, while the 2θ angles of the precipitate phase of Al_3Mg_2 are apparent at the same angles.

REFERENCES

1. C. Saravanan, K. Subramanian, V. A. Krishnan, and R. S. Narayanan, Effect of particulate reinforced aluminium metal matrix composite–a review, Mechanics and Mechanical Engineering, 19(1) (2015) 23-30.

2. V. Kishan, A. Devaraju, and K.P. Lakshmi, Influence of volume percentage of NanoTiB2 particles on tribological & mechanical behaviour of 6061-T6 Al alloy nano-surface composite layer prepared via friction stir process,

3. R. Pandiyarajan, P. Maran, S. Marimuthuand, and K. C. Ganesh, Mechanical and tribological behavior of the metal matrix compositeAA6061/ZrO2/C, J. Mechan. Sci. Technol. 31 (10) (2017) 4711–4717.

4. Girija Moonaa, R.S. Walia, Vikas Rastogi, and Rina Sharma, Aluminium metal matrix composites: a retrospective investigation, Indian J. Pure Appl. Phys. 56 (2018) 164–175.

5. Q. Liu, L. Ke, F. Liu, C. Huang, and L. Xing, Microstructure and mechanical property of multi-walled carbon nanotubes reinforced aluminum matrix composites fabricated by friction stir processing, Materials & Design, 45 (2013) 343-348.

6. Z. Ma, Friction stir processing technology: a review, Metallurgical and materials Transactions A, 39(3) (2008) 642-658.

7. S. K. Karna, D. R. V. Singh, and D. R. Sahai, Application of Taguchi method in indian industry, International Journal of Emerging Technology and Advanced Engineering, 2(11) (2012) 387-391.

8. Y. Kwon, I. Shigematsu, and N. Saito, Mechanical properties of fine-grained aluminum alloy produced by friction stir process, Scripta Materialia, 49(8) (2003) 785-789.

9. S. Wenlai and D. D. L. Chung, "Fabrication of particulate aluminum matrix composites by liquid metal infiltration," J. Mat. Sci., vol. 29, pp. 3128-3150, 1994.

10. S. Das, "Development of aluminum alloy composite for engineering applications," Trans. Indian Inst. Met., vol. 57, no. 4, pp. 325-334.,August 2004.

11. M. K. Abbass, E. K. I Brahim, and E. S. Noeem, "Effect of heat treatments on the mechanical properties and wear resistance of Al alloy matrix composite," J. of Engineering and Technology,University of Technology, Baghdad, vol. 29, no. 12, pp. 518-533, 2011.

12. K. Elangovan, and V. Balasubramanian, Influences of tool pin profile and tool shoulder diameter on the formation of friction stir processing zone in AA6061 aluminium alloy, Materials & design, 29(2) (2008) 362-373.

13. Muna K. Abbass, and Noor Alhuda B. Sharhan. Optimization of Friction Stir Processing Parameters for Aluminum Alloy (AA6061-T6) Using Taguchi Method. Al-Qadisiyah Journal for Engineering Sciences 12 (2019), pp1-6.

14. Namdev Ashok Patil, Srinivasa Rao Pedapati, Othman Bin Mamat and Abdul Munir Hidayat Syah Lubis. Optimization of Friction Stir Process Parameters for Enhancement in Surface Properties of Al 7075-SiC/Gr Hybrid

Surface Composites. Coatings Journal ,2019, 9, 830, pp.1-17; doi:10.3390/coatings9120830 , www.mdpi.com/journal/coatings.

15. Muna K. Abbass and Jihad G. Abdul-Qader. Effect of friction stir processing one microstructure and mechanical properties of TIG welded aluminum alloy 2024T3. Test Engineering and Management, Mechanical Engineering, (2020)

16. M. M. El-Rayes, and E. A. El-Danaf, The influence of multi-pass friction stir processing on the microstructural and mechanical properties of Aluminum Alloy 6082, Journal of Materials Processing Technology, 212(5) (2012) 1157-1168.

17. Ibrahim H. Zainelabdeen, Fadi A. Al-Badour, Akeem Yusuf Adesina, Rami Suleiman and Fadi A. Ghaith," Friction stir surface processing of 6061 aluminum alloy for superior corrosion resistance and enhanced microhardness", International Journal of Lightweight Materials and Manufacture, Volume 6, (March 2023) , PP. 129-139.

18. M. Barati, M. Abbasi and M. Abedini."The effects of friction stir processing and friction stir vibration processing on mechanical, wear and corrosion characteristics of Al6061/SiO2 surface composite."Journal of Manufacturing Processes Volume 45, September 2019, Pages 491-497.

FINANCING

CONFLICT OF INTEREST
All authors reviewed the results, approved the final version of the manuscript and agreed to publish it.

AUTHORSHIP CONTRIBUTION
Conceptualization: Khaldoon K. Jlood, Muna K. Abbass, Mahdi M. Hanoon.
Data curation: Khaldoon K. Jlood, Muna K. Abbass, Mahdi M. Hanoon.
Formal analysis: Khaldoon K. Jlood, Muna K. Abbass, Mahdi M. Hanoon.
Research: Khaldoon K. Jlood, Muna K. Abbass, Mahdi M. Hanoon.
Methodology: Khaldoon K. Jlood, Muna K. Abbass, Mahdi M. Hanoon.
Drafting - original draft: Khaldoon K. Jlood, Muna K. Abbass, Mahdi M. Hanoon.
Writing - proofreading and editing: Khaldoon K. Jlood, Muna K. Abbass, Mahdi M. Hanoon.